Clin Oral Invest (2015) 19:2015–2025
DOI 10.1007/s00784-015-1412-9

ORIGINAL ARTICLE

Niobium pentoxide as radiopacifying agent of calcium silicate-based material: evaluation of physicochemical and biological properties

Guilherme F. Silva · Mário Tanomaru-Filho · Maria I. B. Bernardi · Juliane M. Guerreiro-Tanomaru · Paulo S. Cerri

Received: 17 September 2014 / Accepted: 21 January 2015 / Published online: 3 February 2015

Abstract
Objectives The physicochemical properties and the tissue reaction promoted by microparticulated or nanoparticulated niobium pentoxide (Nb_2O_5) added to calcium silicate-based cement (CS), compared to MTA-Angelus™, were evaluated.
Materials and methods Materials were submitted to the tests of radiopacity, setting time, pH, and calcium ion release. Polyethylene tubes filled with the materials were implanted into rats subcutaneously. After 7, 15, 30, and 60 days, the specimens were fixed and embedded in paraffin. Hematoxylin & eosin (H&E)-stained sections were used to compute the number of inflammatory cells (IC). Interleukin-6 (IL-6) detection was performed, and the number of immunolabeled cells was obtained; von Kossa method was also carried out. Data were subjected to ANOVA and Tukey test ($p \leq 0.05$).
Results Nb_2O_5micro and Nb_2O_5nano provided to the CS radiopacity values (3.52 and 3.75 mm Al, respectively) superior to the minimum recommended. Groups containing Nb_2O_5 presented initial setting time significantly superior than mineral trioxide aggregate (MTA). All materials presented an alkaline pH and released calcium ions. The number of IC and IL-6 immunolabeled cells in the CS+Nb_2O_5 groups was significantly reduced in comparison to MTA in all periods. von Kossa-positive structures were observed adjacent to implanted materials in all periods.
Conclusions The addition of Nb_2O_5 to the CS resulted in a material biocompatible and with adequate characteristics regarding radiopacity and final setting time and provides an alkaline pH to the environment. Furthermore, the particle size did not significantly affect the physicochemical and biological properties of the calcium silicate-based cement.
Clinical relevance Niobium pentoxide can be used as radiopacifier for the development of calcium silicate-based materials.

Keywords Mineral trioxide aggregate · Calcium silicate cement · Biocompatibility · Physicochemical properties · Radiopacifiers

G. F. Silva · M. Tanomaru-Filho · J. M. Guerreiro-Tanomaru
Department of Restorative Dentistry, UNESP-Univ. Estadual Paulista, Dental School, Araraquara, SP, Brazil

M. I. B. Bernardi
Physics Institute of São Carlos, Grupo Crescimento de Cristais e Materiais Cerâmicos, University of São Paulo-USP, São Carlos, SP, Brazil

P. S. Cerri
Laboratory of Histology and Embryology, UNESP-Univ. Estadual Paulista, Dental School, Araraquara, SP, Brazil

P. S. Cerri (✉)
Department of Morphology-Laboratory of Histology and Embryology, UNESP-Univ Estadual Paulista, Dental School, Rua Humaitá, 1680, Centro, CEP, 14801-903 Araraquara, SP, Brazil
e-mail: pcerri@foar.unesp.br

Introduction

Treatment of communications between the root canal and external surface, such as radicular perforation and root-end cavities, is one of the most difficult endodontic proceedings. The prognosis depends in part on the sealing material, which should present satisfactory physicochemical and biological properties. The material is placed on direct contact with the vital tissues, and the reaction induced by its released substances may influence the outcome of treatment.

Calcium silicate-based materials (CS), such as mineral trioxide aggregate (MTA), have been widely used in dentistry

for different applications, including restoration of deep carious lesions, pulp capping and pulpotomy, sealing of root or furcation perforations, filling of internal or external resorption, apexification, and root-end filling in endodontic surgery [1–3]. It has been shown that these materials present biocompatibility, bioactivity, and adequate physicochemical properties regarding to setting time, pH, and releasing of calcium ions [4–8].

MTA Angelus™ is, basically, composed of Portland cement (80 %) and bismuth oxide (20 %), a radiopacifying agent. It has been reported that the value of MTA radiopacity ranges between 4.5 and 8 mm Al [9, 10] and, therefore, has adequate radiopacity according to the standards by ISO 6876 [11]. However, it is well documented that the interaction between bismuth oxide (Bi_2O_3) and the Portland cement (PC) in the hydrated paste interferes in the compressive strength of MTA [12, 13]. The association of Bi_2O_3 changes the microstructure of the cement promoting flaws within the cement [12, 14] and, consequently, increases the porosity and solubility of Portland cement, culminating in the reduction of its resistance [12, 13].

In addition, there is evidence that MTA exhibits higher solubility than the recommended by ANSI/ADA [15] to the root-end filling materials [3]; it has been also demonstrated that MTA Fillapex presents high solubility over time as a root canal filling [8]. Another disadvantage frequently associated to Bi_2O_3, is regarding to its biocompatibility. Studies have reported that bismuth oxide inhibits cellular proliferation of the dental pulp [16] and periodontal ligament [17]. On the other hand, an in vitro study demonstrated that deleterious effect of Bi_2O_3 on human marrow stromal cells was reduced due to the increased thickness of the Ca-P coating on the cement over time [6].

So, attempts to incorporate another material to CS, including nanoparticulated agents, as alternative to Bi_2O_3 have been made [10, 18]. Niobium is a transition metal and has the atomic number 41. This metal has been studied to enhance mechanical properties in titanium alloys of osseointegrated implants due to its resistance to corrosion and its biocompatibility. Moreover, it has been suggested that niobium may stimulate the hydroxyapatite deposition [19]. The use of niobium pentoxide (Nb_2O_5) as a radiopacifying agent of dental materials has been studied. The addition of Nb_2O_5 to an experimental methacrylate-based root canal sealer promoted satisfactory physicochemical properties with increase of radiopacity and microhardness of the material [20, 21].

Despite these recent researches, the influence of Nb_2O_5 on the properties of calcium silicate-based cements with consistency to be used as root-end filling materials is unknown. Therefore, the aim of this study was to evaluate the physicochemical and biological properties of microparticulated or nanoparticulated Nb_2O_5 added to calcium silicate-based cement in comparison to commercially available MTA.

Materials and methods

The materials evaluated in the present study were as follows: calcium silicate-based cement (White Portland cement; CPB-40—Votorantim Cimentos, Camargo Correa S.A., Pedro Leopoldo, MG, Brazil) with microparticulated niobium pentoxide, CS+Nb_2O_5micro group; calcium silicate-based cement with nanoparticulated niobium pentoxide, CS+Nb_2O_5nano group; and mineral trioxide aggregate (white MTA-Angelus, Londrina, PR, Brazil; lot. n°. 14414), MTA group. The powder of micro- and nanoparticulated Nb_2O_5 was previously sterilized by ultraviolet method for 30 min. A ratio of 30 % Nb_2O_5 and 70 % CS by weight was used for analyses. MTA and CS+Nb_2O_5micro group were mixed at a ratio of 1 g powder of cement per 0.3 mL liquid (distilled water). Regarding CS+Nb_2O_5nano, it was prepared using a powder:liquid mixing ratio of 1 g:0.33 mL (standardized in pilot tests) because it provided a thicker consistency and, therefore, is adequate for a cement intended for use as a root-end filling material.

Nanoparticulated Nb_2O_5 was prepared by polymeric precursor method at Institute of Physics of São Carlos (University of São Paulo, São Carlos, Brazil), and the particle size obtained was 83 nm, confirmed by Brunauer-Emmett-Teller (BET) surface area analysis. The nanoparticulated Nb_2O_5 was prepared by dissolving of niobium ammonium oxalate {$NH4[NbO(C_2O_4)_2(H_2O)](H_2O)N$} (CBMM, Companhia Brasileira de Metalurgia e Mineração, MG, Brazil) in distilled water, followed by addition of ammonium hydroxide resulting in precipitated niobium hydroxide. This solution was filtered, and citric acid (CA) was added ([CA]/[Nb]=3) and subsequently filtered. The niobium content in the solution was precisely determined by gravimetric analysis. The solution was stirred for 2 h at 70 °C to promote the complex reaction. Ethylene glycol was added to the mixture with mass ratio 60:40. The translucent solution was heated and stirred for several hours. A polymerization process started during the water evaporation, resulting in a highly viscous solution. This resin was heated in an electric furnace at 300 °C for 4 h. The resulting black and soft mass was milled and calcined in an electric furnace for 2 h over alumina slabs at 700 °C [22].

Radiopacity

To determine the radiopacity of the materials, the ISO 6876/2001 standard for dental root-sealing materials [11] was followed to prepare the specimens. Five specimens measuring 10 mm diameter by 1.0 mm thickness were prepared for each material. The specimens were stored at 37 °C for 24 h, and subsequently, they were positioned on five occlusal radiographic films (Insight-Kodak Comp, Rochester, NY, USA) and exposed, along with an aluminum step wedge with variable thickness (from 2 to 16 mm, in 2 mm increments). A GE-

1000 X-ray unit (General Electric, Milwaukee, WI, USA) operating at 50 kvp, 10 mA, 18 pulses/s, and focus-film distance of 33.5 cm was used. The films were processed in a standard automatic processor (Dent-X 9000, Dent-X, Elmsford, USA). Using the ImageTool 3.0 (UTHSCSA, San Antonio, Texas, USA), the digitized radiographs were analyzed; an equal-density tool was used to identify equal-density areas in the radiographic images. This procedure allowed comparison between the radiographic density of the cements and the radiopacity of the different aluminum step wedge thicknesses. The area corresponding to the specimen was selected in each radiographic image to verify the thickness of the aluminum step wedge detected by the software as equivalent to material's radiographic density. Thus, the radiopacity of the evaluated materials was estimated from the thickness of aluminum (in millimeters) by using a conversion equation. The values recorded for each material were averaged to obtain a single value in millimeter Al.

Setting time

This test was carried out as determined by #57 of American Dental Association (ADA) [15] and C266-03 of American Society for Testing and Materials (ASTM) [23]. Six specimens measuring 10 mm diameter and 2 mm in height were made per each material. At 120±10 s after the onset of mixture, the assembly was placed in a well-sealed plastic flask and stored in an oven at 37 °C and 95 % relative humidity. After 150±10 s to the onset of mixture, a Gilmore needle of 100± 0.5 g and an active tip of 2.0±0.1 mm diameter was vertically placed on the cement surface. This procedure was repeated at 60 s intervals. The initial setting time of the cement was considered as the time between the onset of mixture and the moment when the marks of needles could not be observed on the cement surface. Concerning the final setting time, a Gilmore needle of 456±0.5 g and an active tip of 1.0±0.1 mm diameter was used as previously described. The initial and final setting times were determined by the arithmetic mean of six repetitions of the test for each group.

Analyses of the alkalinizing activity and calcium ion release

pH and calcium ion release were evaluated according to the methodology previously described [18]. Ten polyethylene tubes (Embramed Ind. Com., São Paulo, SP, Brazil) measuring 10.0 mm length and 1.6 mm diameter were filled with freshly prepared samples of each material, sealed in flasks containing 10 mL of distilled water, and stored at 37 °C. After 1 day, the tubes were carefully removed and placed into new flasks with an equal amount of distilled water, and this procedure was repeated after 7, 14, and 28 days. The solution pH was analyzed at each period using a digital pH meter (Ultra-Basic, Denver Instrument Company, Arvada, CO). After pH reading, the calcium ions released in the distilled water were measured with an atomic absorption spectrophotometer (H1170 Hilger & Watts; Rank Precision Industries Ltd. Analytical Division, London, UK) equipped with a calcium hollow-cathode lamp (422.7 nm wavelength and 0.7 nm window) operated at 20 mA. The readings of calcium ion release were compared with a standard curve obtained from multiple dilutions of pure calcium in ultrapure water.

Tissue reaction

The research protocol on animal use of this study was authorized by the Ethical Committee for Animal Research of the São Paulo State University, Brazil (CEUA n° 26/2010-Araraquara Dental School-UNESP). Experiments were performed in thirty-two adult male Holtzman rats (*Rattus norvegicus albinus*) weighing 250±10 g. The rats were maintained in individual stainless steel cages under a 12:12 light-dark cycle at a controlled temperature (23±2 °C) and humidity (55±10 %), with food and water provided ad libitum.

The polyethylene tubes (Embramed Ind. Com., São Paulo, SP, Brazil) with 10.0 mm length and 1.6 mm diameter, previously sterilized with ethylene oxide, were filled with CS+ Nb_2O_5micro, CS+Nb_2O_5nano, or MTA. Immediately, after mixing of the materials, the polyethylene tubes were filled and implanted into the dorsal subcutaneously. In each rat, two polyethylene tubes, filled with different materials each, were implanted subcutaneously. Five polyethylene tubes were analyzed per group in each period.

The animals were anesthetized with intraperitoneal injection of ketamine (80 mg/kg of body weight) combined with xylazine (4 mg/kg of body weight). The dorsal skin was shaved and disinfected with 5 % iodine solution. Subsequently, a 20-mm-long incision was made using a scalpel (n° 15, Fibra Cirúrgica, Joinville, SC, Brazil) and two polyethylene tubes, each filled with one of the materials, were placed into the subcutaneous pockets. After 7, 15, 30, and 60 days of implantation, the tubes surrounded by connective tissue were removed, and the specimens were processed for paraffin embedding.

Histological procedures

The specimens were fixed for 48 h at room temperature in 4 % formaldehyde (prepared from paraformaldehyde) buffered at pH 7.2 with 0.1 M sodium phosphate. Subsequently, the specimens were dehydrated in graded concentrations of ethanol, clarified in xylene, and embedded in paraffin. Longitudinal sections 6 μm thick were collected onto slides and stained with hematoxylin & eosin (H&E) for morphological analysis; this method stains cell nucleus in blue/purple and cytoplasm in pink [24]. H&E-stained sections were also used to estimate the number of inflammatory cells in the capsule. Sections

were also submitted to the von Kossa histochemical method [25], for detection of calcified structures (in brown/black color) in the capsule adjacent to the implanted materials. Other sections were adhered to silanized slides for immunohistochemical detection of interleukin-6 (IL-6) [26].

Numerical density of inflammatory cells

The numerical density of inflammatory cells (IC) was undertaken using a light microscope (BX51, Olympus, Tokyo, Japan) and an image analysis system (Image-Pro Express 6.0, Olympus), as previously described [26]. In each implant, three H&E-stained sections of the capsule adjacent to the materials were captured at ×695 (Fig 1a, b); the smallest distance between the sections was 100 μm. In each section, a standardized field 0.09 mm^2 of the capsule adjacent to the opening of the tube implanted was analyzed (Fig. 1b), totaling 0.27 mm^2 per implant. In each area, the total number of IC (neutrophils, lymphocytes, plasma cells, and macrophages) was counted using the image analysis system. Thus, the number of inflammatory cells/mm^2 was obtained for each implant.

Immunohistochemical detection of interleukin-6

For antigen retrieval, deparaffinized sections were immersed in 0.001 M sodium citrate buffer pH 6.0 and submitted to microwave oven cycles for 20 min at 90–94 °C. After a cooling-off period, the sections were immersed in 5 % hydrogen peroxide for 20 min. The sections were washed in 0.1 M sodium phosphate buffer (PBS) at pH 7.2 and were incubated for 30 min with 2 % bovine serum albumin (Sigma-Aldrich Chemie, Munich, Germany). Subsequently, the sections were incubated overnight at 4 °C with primary goat antibody anti-IL-6 (Santa Cruz Biotechnology, Santa Cruz, USA), diluted 1:400. After washings in PBS, the immunoreaction was detected by the labeled streptavidin-biotin system (LSAB-plus kit; Dako, Carpinteria, USA). After incubation for 20 min at room temperature with multi-link solution containing biotinylated mouse/rabbit/goat antibodies, the sections were washed in PBS and subsequently were incubated with streptavidin-peroxidase complex for 20 min at room temperature. Peroxidase activity was revealed by Betazoid DAB (Biocare Medical, Concord, USA) for 3 min; the sections were counterstained with Carazzi's hematoxylin. As negative controls, the primary antibody was replaced by nonimmune serum.

Numerical density of IL-6 immunolabeled cells

In five implants of each group per period, a standardized area (0.09 mm^2) of each section was captured using an Olympus camera (DPI) attached to a light microscopy (BX51, Olympus, Tokyo, Japan) at 695× magnification. The number of immunolabeled cells was computed using an image analysis system (Image-Pro Express 6.0, Olympus). For each tube implanted, the IL-6-positive cells were counted in a standardized area (0.09 mm^2); in each group (n=5), the values were divided by the total area, and then, the number of IL-6/mm^2 was obtained.

von Kossa histochemical reaction

The von Kossa method was used for detection of calcium salt structures (brown/black color) in the capsule juxtaposed to the materials [25]. Three sections per implant were selected at intervals of at least 100 μm. Deparaffinized sections were immersed in 5 % silver nitrate solution for 1 h; the sections were washed in distilled water and subsequently were immersed in 5 % sodium thiosulfate for 5 min. After washings, the sections were stained by picrosirius method and mounted in resinous medium. As positive control, the sections of tibiae of young rats were used.

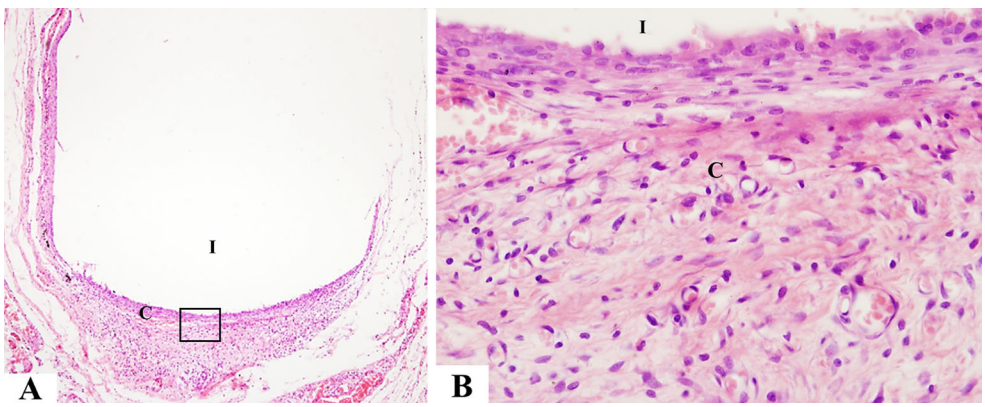

Fig. 1 Light micrographs showing section of a capsule surrounding the polyethylene tube implanted subcutaneously. The letter *I* indicates the space occupied by the material (inside of polyethylene tube), which was removed for obtaining of the histological section. **1a** An overview of the capsule (*C*) adjacent to the opening of the tube implanted, ×20. **1b** High magnification of the outlined area in **1a** shows the standardized area of the capsule (*C*) used to estimate the number of inflammatory cells. ×200, H&E

Statistical analysis

The differences between the groups were statistically analyzed by the SigmaStat 2.0 software (Jandel Scientific, Sausalito, CA). The data of all physicochemical tests and of the morphometrical findings were submitted to ANOVA and Tukey test. The accepted significance level was $p \leq 0.05$.

Results

Radiopacity and setting time

According to Table 1, the radiopacity exhibited by CS+Nb_2O_5micro (3.52 mm Al) and CS+Nb_2O_5nano (3.75 mm Al) was significantly lower in comparison to the MTA (4.73 mm Al); significant differences were not found between CS+Nb_2O_5micro and CS+Nb_2O_5nano. A significant increase in initial setting time was observed in the CS+Nb_2O_5micro and CS+Nb_2O_5nano when compared to MTA. However, statistical differences were not observed among the groups in the values of the final setting time.

Analyses of the pH and calcium ion release

As shown in Table 2, the distilled water containing the materials presented alkaline pH. In all periods, statistical significant differences in the pH values were not observed among the materials analyzed except for CS+Nb_2O_5nano which had a higher value at 14 days. After 28 days, significant reduction in the pH values was observed in all materials.

Regarding calcium ion release, all materials were able to release calcium ions; the lowest values were observed in the period of 1 day. The solutions containing CS+Nb_2O_5micro and CS+Nb_2O_5nano exhibited significantly lower release of calcium ion when compared to MTA, except at 14 days; in this period, significant difference between CS+Nb_2O_5nano and MTA was not detected. At 7 and 14 days, the amount of calcium ions detected in the solution containing CS+Nb_2O_5nano was significantly higher in comparison with CS+Nb_2O_5micro (Table 2).

Table 1 Means and standard deviations of radiopacity (mm Al) for the initial and final setting times (in minutes) for each material

Materials	Radiopacity	Setting time	
		Initial	Final
CS+Nb_2O_5micro	3.52 (0.12)a	45.8 (3.8)a	158.8 (10.4)a
CS+Nb_2O_5nano	3.75 (0.17)a	47.4 (4.8)a	152.3 (7.3)a
MTA	4.73 (0.44)b	24.7 (4.3)b	161.9 (6.4)a

Different letters (a and b) indicate statistically significant differences ($p \leq 0.05$). Tukey test ($p \leq 0.05$)

Table 2 Means and standard deviations of pH values and calcium ion release (mg/L) for the materials in the evaluation periods

	CS+Nb_2O_5micro	CS+Nb_2O_5nano	MTA
1 day			
pH	10.42 (0.10)a,1	10.42 (0.10)a,1	10.34 (0.23)a,1
Calcium	1.87 (0.85)a,1	2.56 (0.71)a,1	5.54 (1.47)b,1
7 days			
pH	10.09 (0.29)a,1	9.87 (0.19)a,2	10.22 (0.10)a,1
Calcium	4.53 (0.59)a,2	14.56 (3.77)b,2	18.84 (0.82)c,2
14 days			
pH	9.90 (0.17)a,1	10.50 (0.23)b,1	9.96 (0.13)a,1
Calcium	8.33 (1.43)a,3	15.66 (2.22)b,2	15.64 (1.63)b,2
28 days			
pH	9.59 (0.45)a,2	9.57 (0.23)a,2	9.69 (0.18)a,2
Calcium	10.68 (2.43)a,3	7.79 (3.37)a,3	14.53 (3.36)b,2

The comparison among groups in the same period is indicated by letters in the lines; same letters=no statistically significant difference. The comparison among periods is indicated by a number in the columns; same numbers=no statistically significant difference. Tukey test ($p \leq 0.05$)

Tissue reaction

Morphological findings and numerical density of inflammatory cells (IC)

At 7 days, the capsules adjacent to the materials implanted exhibited a moderate inflammatory process. Several lymphocytes and blood vessels were observed throughout the capsule (Fig. 2a–c); occasionally, giant multinucleated cells were also seen (Fig. 2b, c). In this period, the capsules exhibited the highest number of IC; however, a significant reduction in the number of IC was observed in the CS+Nb_2O_5micro group when compared with MTA and CS+Nb_2O_5nano groups (Table 3).

A significant decrease in the number of IC was observed in the capsules from 7 to 15 days; however, significant statistical differences were not detected among the groups in this period (Table 3). The inflammatory process was mainly located in the innermost portion of the capsules adjacent to the implants of CS+Nb_2O_5nano (Fig. 2e) whereas in the MTA and CS+Nb_2O_5micro groups, the IC were distributed throughout the capsule (Fig. 2d, f).

Although significant reduction in the number of IC was observed at 30 days in all groups, the number of inflammatory cells in the capsules of CS+Nb_2O_5micro and CS+Nb_2O_5nano materials was statistically lower than in the MTA group (Fig. 3a–c, Table 3).

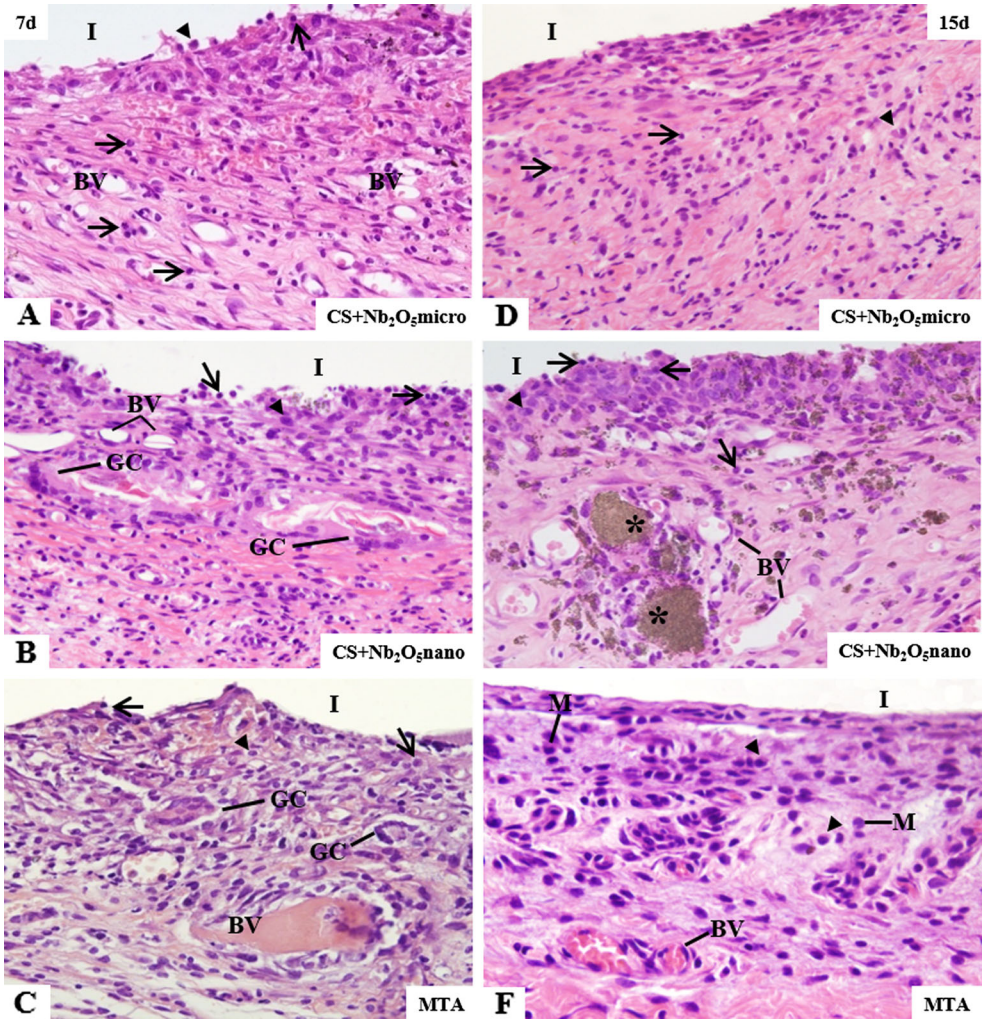

Fig. 2 Light micrographs of sections showing portions of capsule adjacent to the materials implanted in the subcutaneous after **2a–c** 7 days and **2d–f** 15 days. The letter *I* indicates the space occupied by the material (inside of polyethylene tube), which was removed for obtaining of the histological section. **2a** (CS+Nb_2O_5micro—7 days) Numerous inflammatory cells (*arrows*) and blood vessels (*BV*) are present through the thick capsule, ×200. **2b** (CS+Nb_2O_5nano—7 days) Inflammatory cells (*arrows*) and blood vessels (*BV*) are observed in the capsule. Giant cells (*GC*), ×200. **2c** (MTA—7 days) The capsule adjacent to MTA contain various inflammatory cells (*arrows*), some giant cells (*GC*), and blood vessels (*BV*), ×190. **2d** (CS+Nb_2O_5micro—15 days) Inflammatory cells (*arrows*) are situated for the entire capsule, ×190. **2e** (CS+Nb_2O_5nano—15 days) Inflammatory cells (*arrows*) are present, mainly, in the portion of the capsule in close contact to CS+Nb_2O_5nano; particles of material (*asterisks*) are seen among inflammatory cells and blood vessels (*BV*), ×200. **2f** (MTA—15 days) Inflammatory cells, mainly plasma cells (*arrowheads*) and macrophages (*M*), are seen for all the extensions of the capsule. *BV* blood vessels, ×200. *Arrowheads* indicate plasma cells and *M, macrophages.* macrophages. H&E

After 60 days of implantation, the capsules exhibited typical bundles of collagen fibers among fibroblasts and fibrocytes; only few inflammatory cells were seen in the capsules (Fig. 3d–f). Statistically significant differences in the number of inflammatory cells were not detected among the groups (Table 3).

Quantitative analysis of IL-6 immunolabeled cells

Sections submitted to immunohistochemistry for IL-6 detection revealed positive immunolabeling (brown-yellow color) in the cytoplasm of some cells in the capsules, in all periods; however, an enhanced immunolabeling was evident in the capsules at 7 days (Fig. 4a–d, f). According to Table 3, the number of IL-6-positive cells was significantly higher at 7 days; a gradual and significant decrease was seen in the subsequent periods. Significant differences were not seen among the groups at 15 and 30 days. At 60 days, a significant reduction in the number of immunolabeled cells was found in the capsules of CS+Nb_2O_5micro group in comparison to the MTA and CS+Nb_2O_5nano groups. IL-6 immunolabeling was not detected in the negative control sections (data not shown).

Table 3 Number of inflammatory cells (IC) and IL-6 immunolabeled cells per mm^2 in the capsule adjacent to the different materials and control group

	CS+Nb_2O_5micro	CS+Nb_2O_5nano	MTA
7 days			
IC	605.1 (30.6)a,1	687.9 (19.2)b,1	663.3 (35.8)b,1
IL-6	453.3 (14.0)a,1	488.8 (7.8)b,1	488.8 (11.1)b,1
15 days			
IC	578.4 (20.1)a,2	586.5 (17.8)a,2	576.0 (21.3)a,2
IL-6	193.3 (6.0)a,2	197.7 (9.2)a,2	200.0 (11.1)a,2
30 days			
IC	418.2 (12.3)a,3	398.4 (20.7)a,3	452.4 (15.3)b,3
IL-6	124.4 (9.9)a,3	128.8 (9.2)a,3	131.5 (9.4)a,3
60 days			
IC	216.0 (3.3)a,4	216.4 (4.5)a,4	212.3 (10.2)a,4
IL-6	48.8 (7.3)a,4	82.2 (8.5)b,4	89.4 (2.2)b,4

Mean (standard deviation). The comparison among groups ($p<0.05$) is indicated by different letters (a and b) in the lines. The comparison among periods ($p<0.05$) is indicated by numbers in the various columns

von Kossa histochemistry reaction

Examination of sections submitted to von Kossa method exhibited positive structures (brown/black color) in the capsule adjacent to the implanted materials in all periods (Fig. 5a–d, f).

Discussion

It is well documented that Bi_2O_3, used as radiopacifier, interferes in some physicochemical properties and biocompatibility of calcium silicate-based materials [12, 13, 16, 26]. Bi_2O_3 changes the microstructure of the cement promoting flaws within the cement [12, 14] and, consequently, increases the porosity and solubility of the material, culminating in the reduction of its resistance [12, 13]. Other radiopacifying agents have been suggested in the literature. Niobium is a transition metal which has shown satisfactory mechanical and biological properties in titanium alloys of osseointegrated implants [19]. The use of niobium pentoxide (Nb_2O_5), including in the

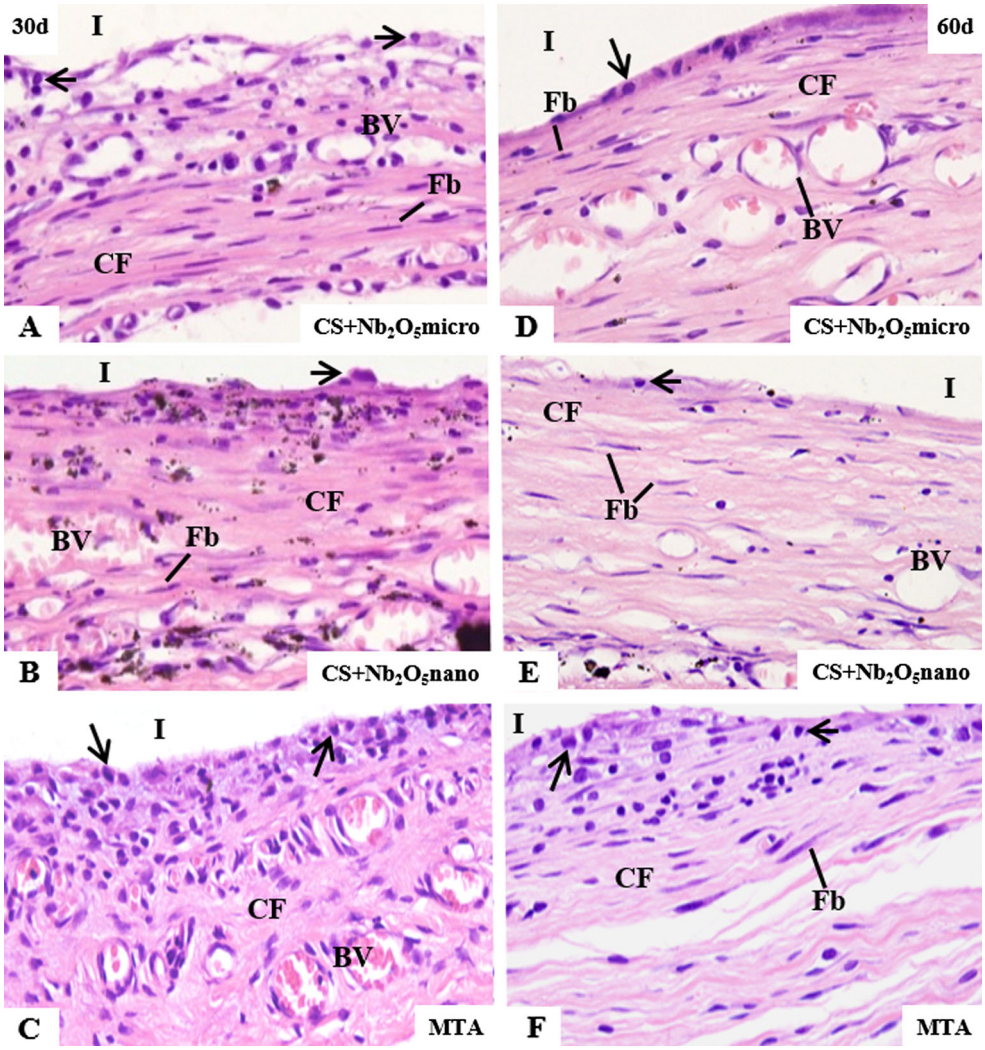

Fig. 3 Light micrographs of sections showing portions of capsule adjacent to the materials implanted in the subcutaneous after **3a**–**c** 30 days and **3d**–**f** 60 days. The letter *I* indicates the space occupied by the material (inside of polyethylene tube), which was removed for obtaining of the histological section. **3a** (CS+Nb_2O_5micro), **3b** (CS+Nb_2O_5nano), **3c** (MTA) The inner portion of the capsule exhibits some collagen fiber bundles (*CF*) among fibroblasts (*Fb*); inflammatory cells (*arrows*) are observed, mainly in close contact with the materials and in the adjacent areas of blood vessels (*BV*), ×190. **3d** (CS+Nb_2O_5micro), **3e** (CS+Nb_2O_5nano), **3f** (MTA) Fibroblasts and fibrocytes (*Fb*) are situated among the collagen fiber bundles (*CF*). Note the presence of some macrophages and lymphocytes (*arrows*) restricted to the surface of the capsule juxtaposed to the materials. *BV* blood vessels, ×200. H&E

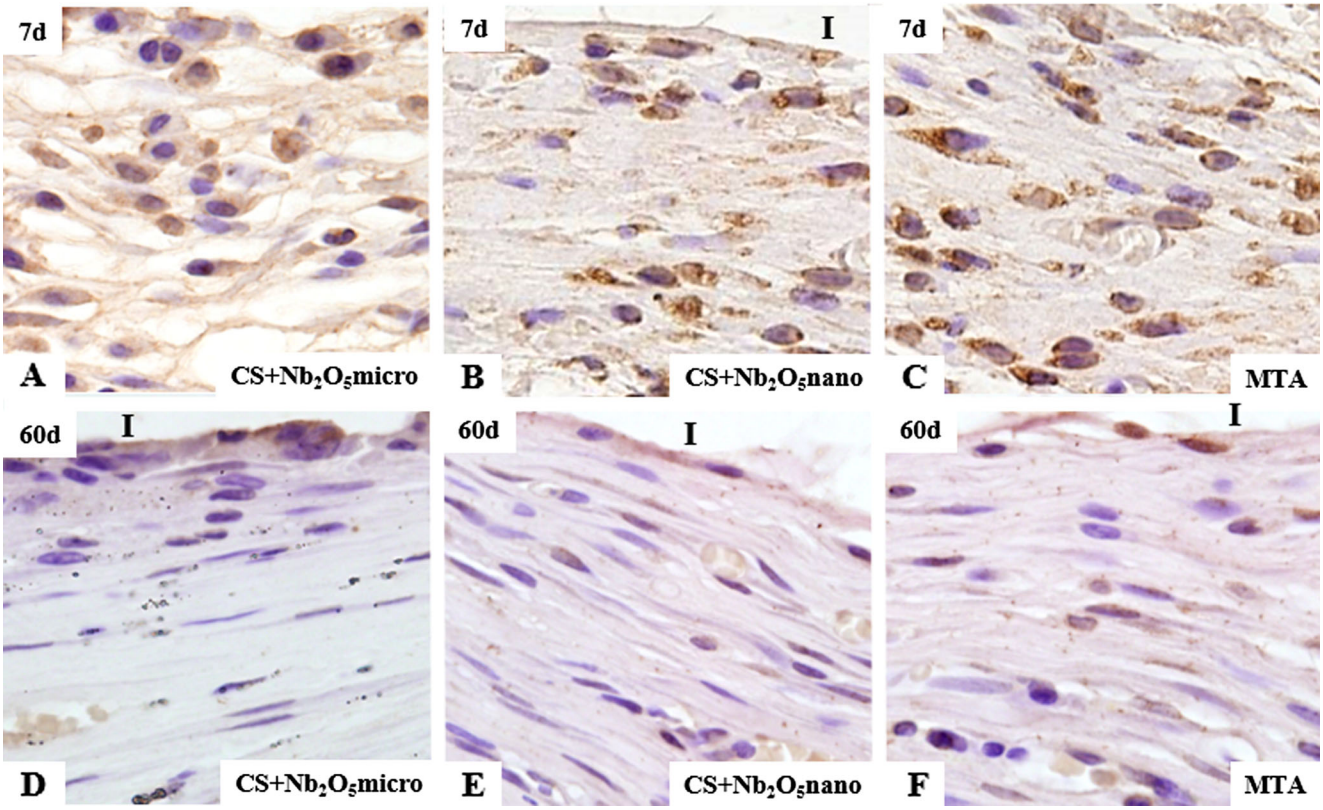

Fig. 4 Light micrographs of sections showing portions of capsule adjacent to the opening of the tubes implanted in the subcutaneous tissue at 7 days (**4a**–**c**) and at 60 days (**4d**–**f**). The sections were submitted to immunohistochemistry for detection of IL-6 and counterstained by hematoxylin. The letter *I* indicates the space occupied by the material (inside of polyethylene tube), which was removed for obtaining of the histological section. IL-6 immunolabeling (*brown-yellow color*) is observed in the cells of the capsule adjacent to the materials. *BV* blood vessel, ×500

nanoparticuled form, as a radiopacifying agent of dental materials has shown promising characteristics [20–22]. Despite this, its influence on the properties of CS cements with thicker consistency to be used, for example, as pulp capping and root-end filling materials, is yet unknown.

Our findings indicated that microparticulated and nanoparticulated niobium oxide provides satisfactory physicochemical and biological properties when added to CS. In this study, the higher proportion of niobium oxide (30 %) added to the CS in comparison to the amount of Bi_2O_3 (20 %) in MTA was performed in the attempt to compensate the lower atomic number of niobium (41—atomic number) than bismuth (83—atomic number). The addition of 30 % microparticulated or nanoparticulated Nb_2O_5 provided to the CS a radiopacity superior to the minimum value recommended to dental materials [27]; however, these values were lower than those presented by MTA. The MTA presented average value around 4.73 mm Al, which is similar to previous studies that reported values ranging to 4.5–8 mm Al [9, 10].

The addition of micro- and nanoparticulated Nb_2O_5 to CS promoted significant increase in the initial setting time in comparison to MTA; however, statistical differences were not observed in the final setting time among the groups. The setting time values of MTA obtained in the present study are in agreement with previous studies, which have reported an initial setting time ranging from 15.5 to 40 min [13, 18, 27, 28]. Furthermore, it has been reported that MTA exhibits final setting time varying from 105 to 168 min [13, 27, 28]. It has been demonstrated that cements with longer setting time are more prone to dissolution during endodontic surgery, whereas those with extremely short setting times might pose technical difficulties during clinical application [18].

The results indicated that all materials presented an alkaline pH in the analyzed periods. This alkalinity occurs due to the formation of calcium hydroxide during the hydration reaction of Portland cement, which is the main component of the evaluated materials. Therefore, similar to MTA, the CS+Nb_2O_5micro and CS+Nb_2O_5nano materials when hydrated give rise to calcium hydroxide as a product of the reaction. Soon after, release of calcium hydroxide from the hydrated cement results in the alkalinity of the storage solution [14], as observed in the present study. The values of pH solutions did not exhibit significant difference among the groups, except the CS+Nb_2O_5nano at 14 days. Alkalizing activity of calcium silicate-based materials has been reported by other authors [3, 7, 18]. Gandolfi et al. (2013) [7] showed that

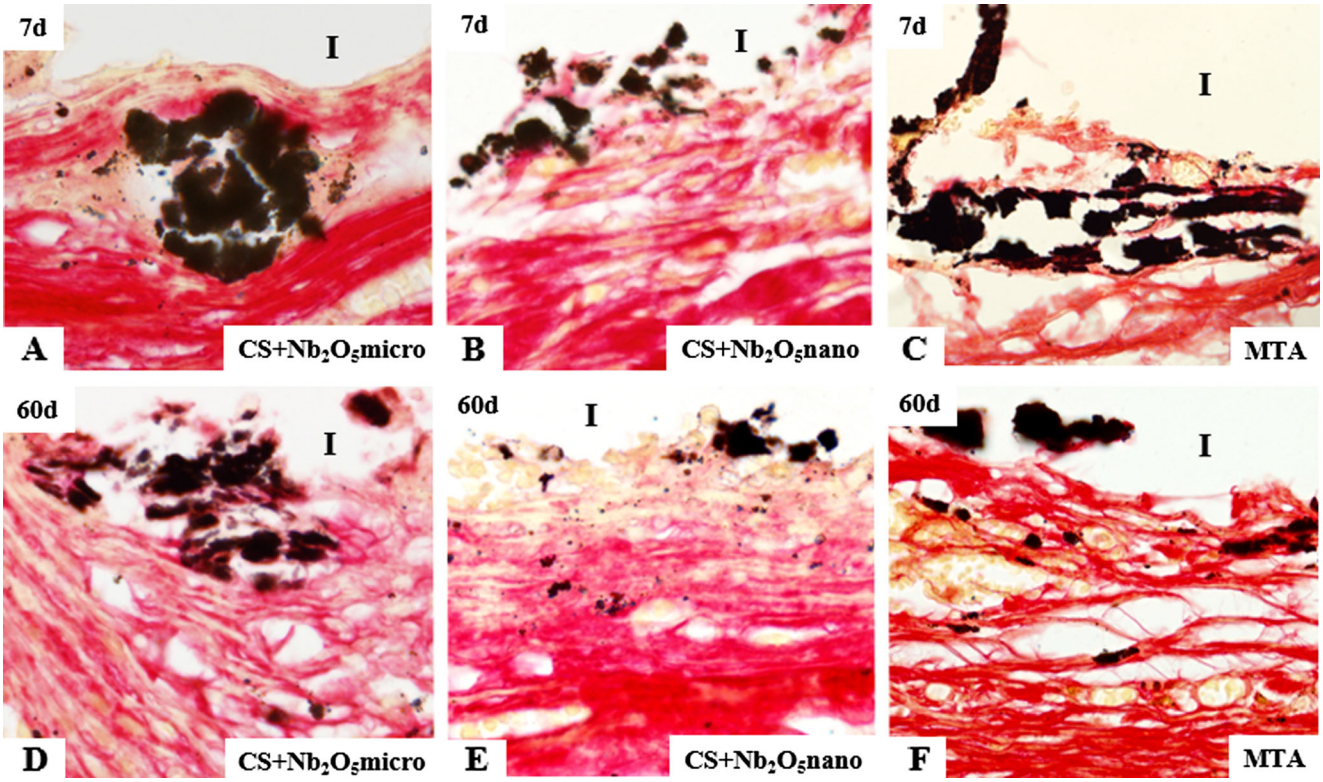

Fig. 5 Light micrographs of sections showing portions of capsule adjacent to the opening of the tubes implanted in the subcutaneous tissue at 7 days (**5a**–**c**) and 60 days (**5d**–**f**). The sections were submitted to the von Kossa reaction and counterstained by picrosirius. The letter *I* indicates the space occupied by the material (inside of polyethylene tube), which was removed for obtaining of the histological section. Small von Kossa-positive structures (*black color*) are dispersed by throughout capsule (**5b**, **e**, **f**). In (**5a**, **c**, **d**), von Kossa-positive structures with irregular shaped are present in the capsules adjacent to the implanted materials, ×250

MTA-based materials significantly increased the pH of the solution, mainly in the initial periods from 3 h to 7 days.

The mechanism of calcium hydroxide formation, from the hydration of Portland cement, may also explain the results found in the test of calcium ion release since all materials were able to release calcium ions. However, the addition of niobium oxide to the calcium silicate-based material promoted a reduction in the amount of calcium ion release in comparison to MTA. Considering that the distilled water containing MTA exhibited a significant increase in the calcium amount in comparison to the CS containing niobium oxide (micro and nano), it is conceivable to suggest that CS+Nb_2O_5micro as well the CS+Nb_2O_5nano may exhibit a reduced solubility in comparison to the MTA.

The analysis of the implants in the subcutaneous revealed that the association of micro- and nanoparticulated Nb_2O_5 to calcium silicate-based cement promoted a moderate inflammatory reaction. In all groups, the alkaline pH of the materials may be responsible by the highest number of inflammatory cells observed in the capsules at 7 days. There is evidence that alkaline pH stimulates the recruitment of inflammatory cells and the production of inflammatory cytokines [29, 30]. Besides, these materials may release some substances that stimulate the migration of inflammatory cells and differentiation of macrophages and plasma cells, often, observed in the capsules adjacent to the materials [26, 29–31]. Thus, the intensity of the inflammatory process reflects the balance between the reaction products released by materials and cytokines and growth factors produced by cells of the host [29, 30].

Among the cytokines released by host cells, there are evidences that excessive IL-6 levels lead to the development of a chronic inflammatory reaction, and, therefore, it has been suggested that this interleukin plays an important role in the host response [32]. Thus, the significant reduction in the number of inflammatory cells and IL-6 immunolabeled cells in the capsules adjacent to the materials from the 15 days indicates that the CS+Nb_2O_5 (micro and nano) as well as MTA did not exert an irritant effect in the connective tissue for a prolonged period. Moreover, these materials allowed the decline of inflammatory process that was gradually replaced by fibroblasts and fibrocytes between the thick collagen fiber bundles indicating therefore that the evaluated materials are biocompatible. At 60 days, the number of IL-6 immunolabeled cells was significantly reduced in the CS+Nb_2O_5micro in comparison to CS+Nb_2O_5nano and MTA suggesting that nanoparticles did not improve the biocompatibility of the material.

In addition, these materials promoted the deposition of von Kossa-positive structures in the subcutaneous [26, 31, 33]. It has been suggested that these structures are formed from the calcium ions released during the hydration of calcium silicate-based cements such as MTA and Portland cement [3, 7, 31]. The calcium ions can react with carbonate dioxide in the tissues giving rise to calcium carbonate that could act as nucleus of calcification [34]. Although the Nb_2O_5 decreased the amount of calcium ions released by CS materials, the CS+Nb_2O_5micro and CS+Nb_2O_5nano were still able to induce the deposition of von Kossa-positive structures in subcutaneous sites. It is important to emphasize that von Kossa reaction alone is not appropriate for the identification of calcium phosphate phases, and, hence, other techniques should be performed to characterize the chemical nature of the calcified structures [25, 35].

According to the results observed in the present study, radiopacity, setting time, pH, calcium ion release, and tissue reaction were not significantly affected by the particle size (nano- or microparticles). However, the addition of Nb_2O_5nano provided a thicker consistency to the CS becoming its handling and insertion into the tubes easier in comparison to the CS+Nb_2O_5micro and MTA.

Conclusions

With the exception of reduced initial setting time and low calcium ion release, the addition of micro-and nanoparticulated niobium oxide resulted in a material with satisfactory physicochemical and biological properties. Furthermore, the nanoparticulated radiopacifier did not improve the physicochemical and biological properties of calcium silicate-based cement when compared to microparticulated Nb_2O_5. So, additional researches are needed to better comprehension of the interaction between the nanoparticles and the calcium silicate-based cement. Furthermore, studies should be carried out with the purpose to determine the ideal ratio of niobium oxide in calcium silicate-based materials, before its use as radiopacifying agent.

Acknowledgments The authors thank Mr. Pedro Sérgio Simões and Mr. Luis Antonio Potenza for the kind help and technical assistance. This research was supported by FUNDUNESP (Proc. n° 01054/11-DFP), CNPq (Brazil) and CAPES (Brazil).

Conflict of interest The authors declare no conflict of interest.

References

1. Parirokh M, Torabinejad M (2010) Mineral trioxide aggregate: a comprehensive literature review-Part III: clinical applications, drawbacks, and mechanism of action. J Endod 36:400–13
2. Silva GF, Guerreiro-Tanomaru JM, Sasso-Cerri E, Tanomaru-Filho M, Cerri PS (2011) Histological and histomorphometrical evaluation of furcation perforations filled with MTA, CPM and ZOE. Int Endod J 44:100–10
3. Gandolfi MG, Siboni F, Botero T, Bossù M, Riccitiello F, Prati C (2014) Calcium silicate and calcium hydroxide materials for pulp capping: biointeractivity, porosity, solubility and bioactivity of current formulations. J Appl Biomater Funct Mater. doi:10.5301/jabfm.5000201
4. Mitchell PJC, Pitt Ford TR, Torabinejad M, McDonald F (1999) Osteoblast biocompatibility of mineral trioxide aggregate. Biomater 20:167–73
5. Abdullah D, Pitt Ford TR, Papaioannou S, Nicholson J, McDonald F (2002) An evaluation of accelerated Portland cement as a restorative material. Biomater 23:4001–10
6. Gandolfi MG, Ciapetti G, Taddei P, Perut F, Tinti A, Cardoso M, VanMeerbek B, Prati C (2010) Apatite formation on bioactive calcium-silicate cements for dentistry affects surface topography and human marrow stromal cells proliferation. Dent Mater 26:974–92
7. Gandolfi MG, Taddei P, Modena E, Siboni F, Prati C (2013) Biointeractivity-related vs chemi/physisorption-related apatite precursor-forming ability of current root end filling materials. J Biomed Mater Res B 101B:1107–23
8. Vitti RP, Prati C, da Silva EJNL, Sinhoreti MAC, Zanchi CH, de Sousa E, Silva MG, Ogliari FA, Piva E, Gandolfi MG (2013) Physical and chemical properties of MTA Fillapex sealer. J Endod 39:915–18
9. Tanomaru-Filho M, Silva GF, Duarte MAH, Gonçalves M, Guerreiro-Tanomaru JM (2008) Radiopacity evaluation of root-end filling materials by digitization of images. J Appl Oral Sci 16:376–9
10. Camilleri J, Gandolfi MG (2010) Evaluation of the radiopacity of calcium silicate cements containing different radiopacifiers. Int Endod J 43:21–30
11. International Organization for Standardization. ISO 6876: dental root sealing materials. Geneva: The Organization; 2001.
12. Coomaraswamy KS, Lumley PJ, Hofmann MP (2007) Effect of bismuth oxide radiopacifier content on the material properties of an endodontic Portland cement–based (MTA-like) system. J Endod 33:295–8
13. Antonijevic D, Medigovic I, Zrilic M, Jokic B, Vukovic Z, Todorovic L (2014) The influence of different radiopacifying agents on the radiopacity, compressive strength, setting time, and porosity of Portland cement. Clin Oral Investig 18:1597–604
14. Camilleri J (2007) Hydration mechanisms of mineral trioxide aggregate. Int Endod J 40:462–70
15. American National Standard. American Dental Association Specification n° 57 for endodontic filling materials. Chicago: ADA; 1984.
16. Min KS, Kim HI, Park HJ, Pi SH, Hong CU, Kim EC (2007) Human pulp cells response to Portland cement in vitro. J Endod 33:163–6
17. Kim EC, Lee BC, Chang HS, Lee W, Hong CU, Min KS (2008) Evaluation of the radiopacity and cytotoxicity of Portland cements containing bismuth oxide. J Endod 105:e54–e57
18. Duarte MAH, Minotti PG, Rodrigues CT, Zapata RO, Bramante CM, Tanomaru Filho M, Vivan RR, Gomes de Moraes I, Bombarda de Andrade F (2012) Effect of different radiopacifying agents on the physicochemical properties of white Portland cement and white mineral trioxide aggregate. J Endod 38:394–7
19. Denry IL, Holloway JA, Nakkula RJ, Walters JD (2005) Effect of niobium content on the microstructure and thermal properties of fluorapatite glass-ceramics. J Biomed Mater Res Part B: Appl Biomater 75B:18–24
20. Leitune VC, Collares FM, Takimi A, de Lima GB, Petzhold CL, Bergmann CP, Samuel SM (2013) Niobium pentoxide as a novel filler for dental adhesive resin. J Dent 41:106–13

21. Leitune VC, Takimi A, Collares FM, Santos PD, Provenzi C, Bergmann CP, Samuel SM (2013) Niobium pentoxide as a new filler for methacrylate-based root canal sealers. Int Endod J 46: 205–10
22. Viapiana R, Flumignan DL, Guerreiro-Tanomaru JM, Camilleri J, Tanomaru-Filho M (2014) Physicochemical and mechanical properties of zirconium oxide and niobium oxide modified Portland cement-based experimental endodontic sealers. Int Endod J 47: 437–48
23. American Society for Testing and Materials (2000) Standard test method for time and setting of hydraulic-cement paste by Gilmore needles, ASTM C266–03. ASTM, Philadelphia
24. Carazzi D (1911) Eine neue Hämatoxylinlösung. Zeitschrift für wissenschaftliche Mikroskopie und für mikrosko-pische. Technik 28:273
25. Meloan SN, Puchtler H (1985) Chemical mechanisms of staining methods. Von Kossa technique: what von Kossa really wrote and a modified reaction for selective demonstration of inorganic phosphates. J Histotechonol 1:11–3
26. Silva GF, Bosso R, Ferino RV, Tanomaru-Filho M, Bernardi MI, Guerreiro-Tanomaru JM, Cerri PS (2014) Microparticulated and nanoparticulated zirconium oxide added to calcium silicate cement: evaluation of physicochemical and biological properties. J Biomed Mater Res Part A 102A:4336–45
27. Cutajar A, Mallia B, Abela S, Camilleri J (2011) Replacement of radiopacifier in mineral trioxide aggregate; characterization and determination of physical properties. Dent Mater 27:879–91
28. Islam I, Chng HK, Yap AUJ (2006) Comparison of the physical and mechanical properties of MTA and Portland cement. J Endod 32: 193–7
29. Shahi S, Rahimi S, Yavari HR, Mokhtari H, Roshangar L, Abasi MM, Sattari S, Abdolrahimi M (2010) Effect of mineral trioxide aggregates and Portland cements on inflammatory cells. J Endod 36:899–903
30. Vosoughhosseini S, Lotfi M, Shahi S, Baloo H, Mesgariabbasi M, Saghiri MA, Zand V, Rahimi S, Ranjkesh B (2008) Influence of white versus gray mineral trioxide aggregate on inflammatory cells. J Endod 34:715–17
31. Viola NV, Guerreiro-Tanomaru JM, Silva GF, Sasso-Cerri E, Tanomaru-Filho M, Cerri PS (2012) Morphological and morphometric analysis of the biocompatibility of an experimental MTA sealer. J Biomed Mater Res Part B, Appl Biomater 100B:1773–81
32. Nibali L, Fedele S, D'Aiuto F, Donos N (2012) Interleukin-6 in oral diseases: a review. Oral Dis 18:236–46
33. Gomes-Filho JE, Watanabe S, Bernabe PFE, Costa MTM (2009) A mineral trioxide aggregate sealer stimulated mineralization. J Endod 35:256–60
34. Seux D, Couble ML, Hartmann DJ, Gauthier JP, Magloire H (1991) Odontoblast-like cytodifferentiation of human dental pulp cells in vitro in the presence of calcium hydroxide cement. Arch Oral Biol 36:117–28
35. Bonewald LF, Harris SE, Rosser J, Dallas MR, Dallas SL, Camacho NP, Boyan B, Boskey A (2003) von Kossa staining alone is not sufficient to confirm that mineralization in vitro represents bone formation. Calcif Tissue Int 72:537–47